SpaceOps-2020,7,x1482

GNSS-based navigation for a remote sensing three-satellite formation flying

Francesca Scala[a]*, Camilla Colombo[b], Gabriella Gaias[c], Manuel Martìn-Neira[d]

[a] *Department of Aerospace Science and Technology, Politecnico di Milano, Via La Masa 34, 20156, Milano, Italy*, francesca1.scala@polimi.it

[b] *Department of Aerospace Science and Technology, Politecnico di Milano, Via La Masa 34, 20156, Milano, Italy*, camilla.colombo@polimit.it

[c] *Department of Aerospace Science and Technology, Politecnico di Milano, Via La Masa 34, 20156, Milano, Italy*, gabriella.gaias@polimi.it

[c] *Department of Aerospace Science and Technology, Politecnico di Milano, Via La Masa 34, 20156, Milano, Italy*, Manuel.Martin-Neira@esa.int

* Corresponding Author

Abstract

This paper presents the architecture and the algorithms implemented for the guidance, navigation, and control system of a three-satellite formation flying mission study, the Formation Flying L-band Aperture Synthesis. This mission concept is developed in the remote-sensing field, to improve the performances of Earth observation missions for land and oceans applications. This work aims to provide a high-fidelity tool environment for the simulation of guidance, navigation, and control of the operative phases of the mission. The navigation is based on Global Navigation Satellite System receivers, to provide an accurate absolute and relative state of the satellites in the formation, thanks to the onboard filter. The analysis is integrated with the definition of control algorithms, to provide a commanded control to the onboard low thrust engine actuators. The desired trajectories from the guidance algorithms are used as inputs to define the control effort for the satellites. Moreover, it tackles the stringent accuracy requirements on the real-time relative navigation solution. Accuracy in the order of 2 cm is required for safe guidance and control of the formation. The design and development of these algorithms for the formation-flying scenario are performed with an in-house suite, developed at Politecnico di Milano in the MATLAB/Simulink environment (SkiLLeD suite), based on C++ functions. The proposed analysis provides a simulation environment for formation flying to verify the main operative phases and the performances in terms of the absolute and relative state reconstruction, as well as the control knowledge accuracy. The methodology applies to other multi-satellite missions in similar orbital scenarios, relying on the Global Navigation Satellite System, also considering the recent trend of employing low-thrust engines onboard scientific satellites.

Keywords: Formation flying, Remote sensing, GNC, GNSS navigation

1. Introduction

Distributed missions have increased their importance in the field of Earth observation and remote sensing. Multi-satellite formation flying working as nodes of a network of sensors can enhance the scientific performances, in terms of spatial resolution of the radiometer payloads. Formation flying represents an opportunity to increase the virtual aperture size of the scientific payloads, and, as a result, their spatial resolution [1,2]. For this purpose, the development of guidance, navigation and control system is fundamental for satellites flying as a network of sensors, to design the scientific observation phase of a mission. The need to maintain the satellites at a correct relative distance and orientation is essential to guarantee nominal scientific performances.

In this paper, we present the procedure and the main results for the definition of the Guidance, Navigation and Control (GNC) simulator for a remote sensing formation flying mission in Low Earth Orbit (LEO). This study is part of a new mission concept by the European Space Agency (ESA) devoted to investigating the feasibility of future multi-satellite formation flying missions for interferometry applications. This mission study, the Formation Flying L-band Aperture Synthesis (FFLAS), consists of a three-satellite formation, on a quasi-circular Sun-Synchronous Orbit (SSO) at a nominal altitude of 770 km [3,4]. Since the mission will fly in the LEO region with a nominal inter-satellite distance of 12 m, this may pose challenging conditions for the control and navigation definition of the formation flying.

Specifically, controlling the satellites relative position at the centimetre level is required to maintain a safe formation during the whole duration of the mission. On the other hand, the ground reconstruction of the relative position should be known within millimetre-level precision. So far, several missions demonstrated the feasibility of a precise millimetre relative navigation in LEO [5]. Global Navigation Satellite System (GNSS) based navigation systems were implemented on several occasions, thanks to the possibility to recover information on both the absolute and relative state of the satellites, such as for the on-ground navigation system of GRACE mission [6], the autonomous formation flying system based on a Global Position System (GPS) for both the PRISMA [7] and the TanDEM-X/TerraSAR-X mission [8], and the absolute and relative navigation algorithm of CanX-4/CanX-5 mission [9]. The analyses presented in this paper focus on the definition of a relative navigation system, based on the GNSS and onboard navigation algorithms. Moreover, this analysis is integrated with guidance and control algorithms, to set up a simulation environment for the main mission operational phases. The objective of the analysis is to simulate the performances during the nominal scientific phase of the mission for Earth observation and the scientific payload calibration phase.

For LEO satellites, the first challenge to be considered in the design of navigation algorithms is related to the presence of uncertainties in the carrier phase measurements and to the limited duration time of the continuous positioning signal from one single GNSS satellite. These conditions require proper algorithms and onboard filter development to provide a precise relative navigation reconstruction onboard within the satellites. The possibility to implement a combination of GNSS and vision-based navigation could also be considered to increase the accuracy and the reliability in the position reconstruction [10]. Additional optical sensors could provide accurate measurements of the inter-satellite distance, to be combined by the navigation filter with the GNSS information. In this work, GNSS measurements were considered to design a relative navigation system for the cooperative formation flying of FFLAS.

A second challenge is related to the level of achievable accuracy, which depends on several factors, such as the complexity of the system, the onboard algorithm, the hardware availability, etc. The considerations from the state-of-the-art available technologies are included in the discussion for a proper GNC definition. The control of the formation is implemented with a low thrust engine. This is required by the nominal formation baseline, which needs a continuous control profile to keep a rigid formation - with a fixed relative attitude profile - and safe flight conditions. The algorithms also include the receivers' model to simulate and verify the performances of the formation flying. Following the results achieved by the PRISMA mission [7], two GNSS receivers and an onboard navigation filter, able to process raw measurements are considered to provide both real-time absolute and relative navigation solutions. The aim is to reach accuracy in the order of metre and centimetre level, for onboard absolute and relative navigation, respectively, with the three satellite cooperatively operating. Moreover, the analysis considers the stringent requirement of the FFLAS mission concept on the real-time relative navigation solution, which should be in the order of 1 cm (1-σ). For these reasons, each satellite employs identical hardware and carries out the estimation of both absolute and relative navigation solution. The design and development of the guidance, navigation and control algorithm for formation-flying scenario is performed with an in-house suite, developed at Politecnico di Milano in the MATLAB/Simulink environment (SkiLLeD suite). This allows modelling with high fidelity the formation flying behaviour during mission operations in an environment subject to orbital perturbations. The absolute dynamics of each satellite is propagated in the Earth Mean Equator and Equinox of J2000 (EMEJ2000) inertial reference frame. The relative dynamics is propagated in the framework of the Relative Orbital Elements (ROEs), as well as considering the shape of the relative trajectory in the co-moving radial-transversal-normal (RTN) orbital frame.

The proposed analysis provides a simulation environment for formation flying to verify the main operative phases and the GNC performances of a remote sensing formation mission. The methodology applies to other multi-satellite missions in similar orbital scenarios, relying on the GNSS navigation system, also considering the recent trend of employing low-thrust engines onboard scientific satellites. The relative motion is analysed through high-fidelity simulations to assess the realistic performances of the nominal FFLAS mission operations.

The paper starts with a description of the FFLAS mission concept, in Section 2, describing the geometry of the formation and the main requirements for the GNC system. Then it presents the description of the GNC architecture in Section 3, and the algorithms implemented, in Section 4. The simulation environment is described, with the reference frame description and the orbital dynamic model used in the simulator. Moreover, the implementation in MATLAB/Simulink® of the algorithms for guidance, control and navigation is presented, to provide a baseline environment for the simulation of the operational phases of FFLAS. Finally, Section 5 presents the performances of the simulator in the nominal science mode of the mission. The control for keeping the triangular formation of FFLAS is considered, to maintain the satellites at a fixed relative distance for observation purposes. The absolute and relative position reconstruction from the navigation information, are implemented with the guidance trajectory to provide a commanded control to the onboard actuator. Moreover, the actual control given by the low thrust engines is computed for the closed-loop simulation. Section 6 presents the results and the final considerations after the GNC simulation results for the FFLAS mission study.

2. FFLAS mission description

The FFLAS mission concept is composed of three satellites, flying in formation, at a close distance, as shown in Fig. 1. The satellites have a hexagonal shape, to allocate the remote-sensing payload, an L-band Aperture Synthesis Radiometer, with the aim of combining the information on the thermal radiation from the Earth to produce a map of the Earth surface in terms of different parameters, such as soil moisture or oceans salinity [3].

The three satellites will be injected in a quasi-circular dusk-dawn SSO at 770 km of altitude. After the commissioning and the first formation reconfiguration, the nominal baseline is acquired, with the satellites flying in an equilateral triangular formation (Fig. 1). The nominal size of the triangle is 12.5 m sides, driven by the payloads requirements to gain high-resolution images, of about 10 m [3]. Since the satellites have an external dimension of 8 m in diameter, the close proximity of the nominal science mode poses a great challenge to the GNC system design, in particular for the onboard navigation accuracy. The design of the navigation and control subsystem is driven by the following mission requirements:

- The relative position between the satellites should be controlled within $\pm$ 2 cm (1 sigma) from the nominal value.
- The real-time relative navigation position should be known with $\pm$ 1 cm (1 sigma) accuracy.
- The ground relative position reconstruction should be known with $\pm$ 2 mm (1 sigma) accuracy.

These requirements impact the design of the onboard controller and navigation filter. In particular, the need of including optical sensors in addition to GNSS receivers will be evaluated contextually to the simulation of the mission scenarios. This paper focus on the description of the GNC architecture and algorithms developed for a generic multiple satellite formation flying mission and applied to the FFLAS mission study. The simulator, developed in MATLAB/Simulink® environment, is based on a C++ function for the dynamic description of the satellite motion, to reduce the computational effort during the simulation. The simulation of the nominal science mode of FFLAS is presented in this paper, to evaluate the preliminary results in terms of navigation and control accuracy of the simulator itself.

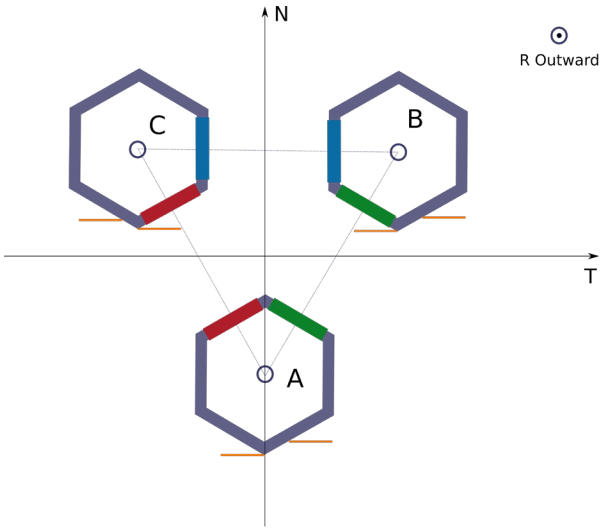

Fig. 1: Nominal formation architecture of the FFLAS formation for the science phase.

3. Guidance, navigation, and control system architecture

The guidance, navigation and control system is designed to provide a simulator tool for a generic multiple satellites formation flying mission. It is based on a distributed real-time filter, onboard each satellite in the formation. It includes GNSS navigation sensors and low thrust engine actuators, to provide an environment for the simulation of the nominal and non-nominal mission operational scenarios, from the launcher deployment to the end-of-life. The satellites share continuously the information on the absolute and relative position reconstruction, via the optical inter-satellite link, and continuously control their position thanks to the low thrust engines.

3.1 Reference frame definitions

The spacecraft dynamics is propagated in the inertial absolute orbital frame, for a high-fidelity inclusion of the orbital perturbation in the LEO environment. The Earth Mean Equator at the J2000 epoch (EMEJ2000) is considered for inertial propagation. Then the propagation is converted into the True-of-Date (ToD), also considering the nutation effect, for computation of the relative dynamics in the RTN frame. Finally, the ROEs framework is computed to describe the relative motion.

3.1.1 Inertial absolute orbital frames

The inertial reference frames have the following characteristics: they are non-rotating with respect to stars and they have a non-accelerating origin, with a velocity typically non-zero, and a negligible acceleration.

The first inertial frame considered in this work is the EMEJ2000 frame. It is defined by the Earth's equatorial plane, where the axis X_{J2000} and Y_{J2000} lye, and by the normal to the mean equator of date at epoch 2000 January 01, 12:00:00, the Z_{J2000} axis. Moreover, the X_{J2000} is defined as the intersection between the equatorial and ecliptic plane (vernal equinox), and Z_{J2000} is approximately in the direction of the Earth's spin axis at the J2000 epoch.

Moreover, we also consider the True od Date (ToD) Earth equator frame, to include the nutation and precession effects. In this system, the x-axis (X_{ToD}) points toward the true vernal equinox at the current epoch, while the z-axis (Z_{ToD}) points toward the true rotation axis at the current epoch. The rotation matrix to pass from the EMEJ2000 to the ToD frame depends on the terrestrial time, the nutation, and the precession effects [11]:

$$\mathcal{R}_{eme2tod} = N_{nut} \cdot P_{prec} \tag{1}$$

Where N_{nut} and P_{prec} are the nutation and precession matrix respectively [11]:

$$\begin{aligned} N_{nut} &= \mathcal{R}_x(-\varepsilon_N - \Delta\varepsilon)\mathcal{R}_z(-\Delta\psi_N)\mathcal{R}_x(\varepsilon) \\ P_{prec} &= \mathcal{R}_z(-z)\,\mathcal{R}_y(\theta)\,\mathcal{R}_z(-\zeta) \end{aligned} \tag{2}$$

Where ε is the mean obliquity of the ecliptic, $\varepsilon_N + \Delta\varepsilon$ and $\Delta\psi_N$ are the nutation angles: the change of the obliquity of the ecliptic during the 18.6-year nodal period of the Moon and the periodic shift of the vernal equinox, respectively. The precession angles z, θ, ζ describes the orientation of the mean equator and equinox at a generic epoch T, with respect to the equator and equinox of J2000.

3.1.2 Relative Orbital Frames

The relative motion is described in both the radial-transversal-normal and in the relative orbital elements' framework. The former is computed from the ToD frame, and it is defined through a vector triad $\boldsymbol{e_R}$, $\boldsymbol{e_T}$, and $\boldsymbol{e_N}$, defined as following from satellite state in $\{X_{ToD}, Y_{ToD}, Z_{ToD}\}$ representation [12]:

$$\begin{aligned} \boldsymbol{e_R} &= \frac{\boldsymbol{r}}{r} \\ \boldsymbol{e_N} &= \frac{\boldsymbol{r} \times \boldsymbol{v}}{|r \times v|} \\ \boldsymbol{e_T} &= \boldsymbol{e_N} \times \boldsymbol{e_T} \end{aligned} \tag{3}$$

Where $\boldsymbol{r}$ and $\boldsymbol{v}$ are the reference position and velocity expressed in the ToD reference frame. The RTN frame is a rotating synodic frame, described by the angular velocity $\boldsymbol{\omega} = n\,\boldsymbol{e_N}$, with n the mean motion of the reference state.

The relative orbital elements describe the orbital elements of each satellite in the formation with respect to the reference orbital elements [13]. They allow a semi-analytical representation of the dynamical model, with a deep insight into the relative motion. They allow an easy representation of the inter-satellite collision avoidance constraint with the eccentricity-inclination vector separation. The ROEs for the satellite j of the formation are composed by the non-dimensional relative semimajor axis δa, the relative mean longitude $\delta\lambda$, the relative eccentricity vector δe and the

relative inclination vector δi: $\{\delta a, \delta\lambda, \delta e_X, \delta e_y, \delta i_x, \delta i_y\}_j$, where the mean longitude is defined as the sum of the relative mean argument of latitude $M - M_c$, the relative argument of perigee $\omega - \omega_c$, and the relative right ascension of the ascending node $\Omega - \Omega_c$ multiplied by the sine of the inclination of the reference orbit i_c: $\delta\lambda = M - M_c + \omega - \omega_c + (\Omega - \Omega_c)\cos i_c$ [13].

3.2 Guidance, navigation, and control architecture

The architecture scheme of the GNC subsystem for each satellite in the formation is shown in Fig. 2. The absolute and relative dynamics are computed with a high-fidelity propagator (see Section 3.3), representative of the ground truth dynamics. Specifically, as shown in Fig. 2, the absolute state of the chief and the deputies is computed both in the EMEJ2000 and in ToD. The information on the state in ToD is used to compute the relative motion in RTN and ROEs, moreover, the orbital elements are recovered during the propagation for further use. The high-fidelity True of Date state is taken as input in the navigation block. The GNSS receiver is simulated adding noise to the ground truth dynamics, related to the actual receiver onboard the satellites. This is used to compute the absolute and relative state as measured by the GNSS receivers. The sensor measurements of the state together with the predicted onboard dynamics are used by the navigation filter, an Extended Kalman Filter (EKF), for absolute and relative state reconstruction. The onboard propagator implements an absolute dynamic with the inclusion of the Earth oblateness term J_2 and the approximation of the drag effect, only. The absolute and relative state estimation is important for the definition of the ideal control effort to be commanded to the actuators. The guidance algorithm computes the reference trajectory, depending on the mission phase, with a convex optimization problem in the relative motion. The difference between the actual estimated relative state and the ideal optimal state from the guidance algorithm represents the error in the relative trajectory, which is the input to the feedback linearization control. The control gain is selected after a parametric analysis on the convergence of the algorithm. The feedback control linearization provides the commanded control to the onboard actuators, the low thrust engine. At this point, the technological limitations of the engine are applied to the command, in terms of thrust limit, on-off delay, and thrust noise. From this analysis, the actual control provided by the low thrust engine is used as the input control law for the high-fidelity dynamic propagator.

This closed-loop guidance, navigation and control could be used to simulate various operative scenarios of a multiple satellite formation flying, based on GNSS navigation sensors. The possibility to include vision-based navigation is discussed in Section 5, after the preliminary outcomes of the simulations. The eventual vision-based sensor will be included in the close loop as an additional input to the EKF, to improve the accuracy of both the relative and absolute state reconstruction from the external measurements.

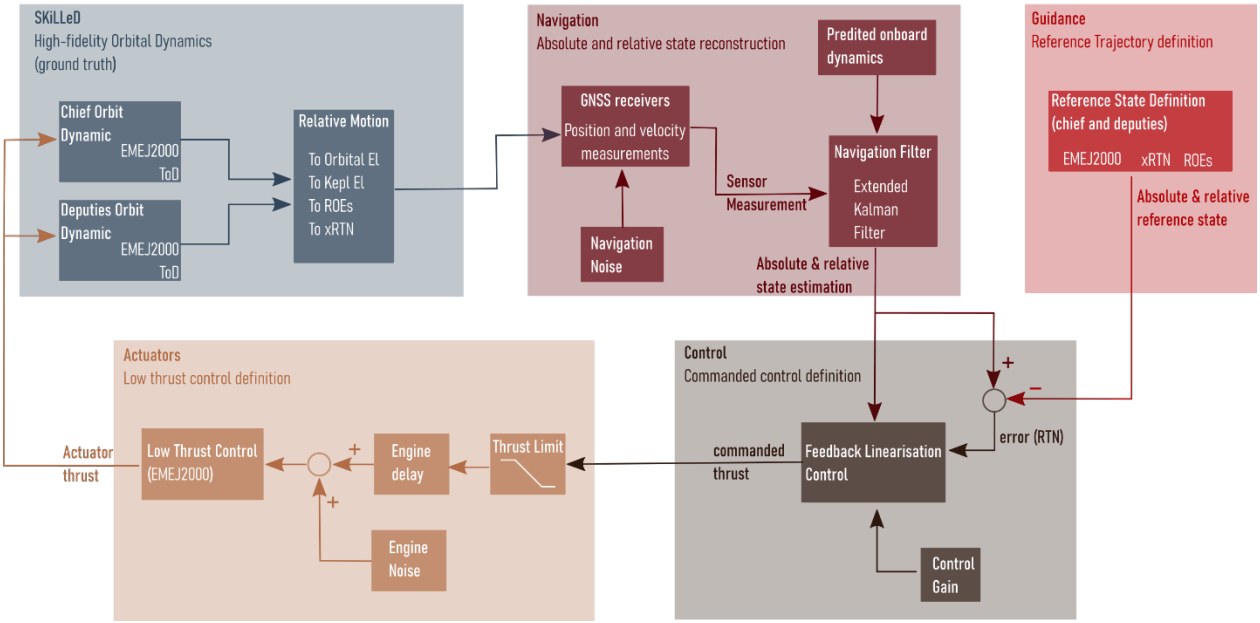

Fig. 2: GNC architecture for the FFLAS formation.

3.3 Orbital dynamics models

The GNC simulator tool is designed to provide a high-fidelity representation of the space environment. This requires the modelling of the relevant disturbing forces acting in the LEO environment, such as the gravity field and the atmospheric drag. These perturbations are included in the integration of the equations of motion, for an accurate description of the absolute state of the satellites.

The absolute orbital dynamic model is propagated in time, also considering the effect of the control acceleration from the Control algorithm. After the propagation of the absolute state, the relative motion is recovered both in the radial-transversal-normal frame and in the relative orbital elements' description. A custom algorithm library was implemented in a C++ environment, to limit the computational effort during the time propagation. This module for the dynamical propagation, called Simulation Kit for Logic Layout Design of Formation Flying (SKiLLeD), was developed at Politecnico di Milano for the MATLAB/Simulink ® environment. The interface between C++ and Simulink is obtained through the MEX function wrapper of MATLAB ® for S-functions. The decision to provide an interface in Simulink is dictated by the need of developing a more user-friendly environment to develop the GNC algorithms. Simulink provides an easy interface for the simulation of the orbital dynamics, which could also include the attitude dynamics and control, in future development.

The SKiLLeD simulator provides a high-fidelity description of the absolute and relative dynamics. The main characteristics of the SKiLLeD tool are reported in Table 1.

Table 1. Inputs, outputs, and orbital perturbations models of SKiLLeD

Inputs	
Timestep	ΔT (sec)
Chief initial condition	$\mathbf{y}_0^C$ (m; m/s)
Deputy i initial conditions	$\mathbf{y}_0^{Di}$ (m; m/s)
Actuator thrust	$\mathrm{T_{eme}}$ (N)
Drag coefficient	$\mathrm{C_D}$
Orbit Perturbations	**Model**
Gravity Field	Grace Earth Gravity Model 02 (GGM02S) (120x120) [14]
Atmospheric Drag	NRLMSISE-02 model [15]
Outputs	
Chief absolute state (ToD)	$\mathbf{y}^{\mathrm{C}}$ (m; m/s) and $\mathbf{kep}^{\mathrm{C}}$ (m, -, rad, rad, rad, rad)
Deputy i absolute state (ToD)	$\mathbf{y}^{Di}$ (m; m/s) and $\mathbf{kep}^{Di}$ (m, -, rad, rad, rad, rad)
Deputy i relative state	$\mathbf{x}_{\mathrm{RTN}}^{i}$ (m)
Deputy i relative orbital el.	$\boldsymbol{\alpha}^{i}$ (–, m, –, –, deg, deg)

The Grace Earth gravity model [14] and the NRLMSISE-02 model [15] are implemented as separated C++ functions, and they are included in the dynamical propagator to compute the absolute state in the EMEJ2000 frame, under the effect of orbital perturbation. Moreover, the structure of the C++ function developed with the possibility to easily include other orbital perturbations in the high-fidelity dynamics, such as the solar radiation pressure and the third body effect.

From the high-fidelity absolute state in EMEJ2000, a conversion is implemented in the model to include the effect of nutation and precession, as described in Section 3.1. The absolute state in ToD is converted into the relative RTN representation via the following rotation matrix:

$$\boldsymbol{\mathcal{R}}_{eme2rtn} = \begin{bmatrix} \boldsymbol{e}_R \\ \boldsymbol{e}_T \\ \boldsymbol{e}_N \end{bmatrix} = \begin{bmatrix} \dfrac{\boldsymbol{r}_{tod}}{|\boldsymbol{r}_{tod}|} \\ \boldsymbol{e}_N \times \boldsymbol{e}_R \\ \dfrac{\boldsymbol{r}_{tod} \times \boldsymbol{v}_{tod}}{|\boldsymbol{r}_{tod} \times \boldsymbol{v}_{tod}|} \end{bmatrix} \tag{4}$$

On the other hand, the ToD states are also converted into the orbital elements for both the chief and the deputies. From the orbital elements, the ROEs can be computed from the osculating elements of the chef (elC) and the deputy (elD) in the form described in Section 3.1.

This procedure allows a precise description of the absolute and relative motion of the satellites in the formation. In particular, the SKiLLeD environment is exploited to provide a high-fidelity ground truth base of the orbital dynamics of the formation flying. These values serve as inputs in the GNC algorithms for the formation performance definition. Fig. 3 shows the high-fidelity propagation of the Keplerian elements and the true-of-date position and velocity for the sun-synchronous reference orbit of FFLAS, for 10 orbital periods.

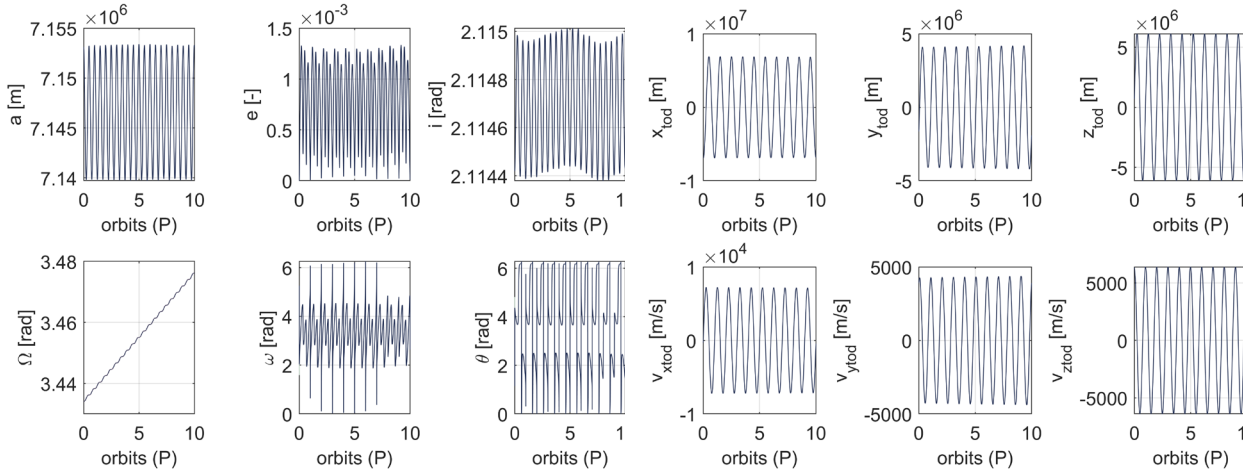

Fig. 3: High-fidelity propagation from SKiLLeD for 20 orbital periods, the Keplerian elements are shown on the left figure, while the true of date position and velocity propagation is on the right.

4. Guidance, navigation, and control algorithm

As described in Section 3, the guidance, navigation and control system is made by navigation algorithms and sensors to determine the satellites trajectory state, moreover, it implements guidance algorithms to determine the desired trajectories, and finally, the control algorithm is included together with the actuator model to perform continuous low thrust control of the formation geometry.

4.1 Guidance algorithms

The guidance algorithm is implemented to provide the simulator with the reference trajectories for different mission scenarios. For the science mode, the reference trajectory is determined from the desired state of the station keeping problem. At each time instant, the algorithm computes the desired state from the relative orbital elements (ROEs) and the inter-satellite collision avoidance state, to maintain a collision-free flight.

The guidance algorithm is based on an optimization problem to determine the optimal trajectory to be followed by the satellites. The formulation is based on the transformation of a classical optimal representation into a convex formulation, to guarantee the existence of a unique optimal solution. Approaches relying on the convex formulation to compute the trajectory for a multiple satellite formation have already been discussed in the literature [16,17], and the reduced computational effort required by the approach is suitable for the implementation on board the satellites, which could have reduced computational capabilities.

The algorithm uses the relative orbital elements to compute the desired relative state of the satellites, including the main constraints to the operations. First, collision avoidance is considered to define a collision-free zone for the satellite manoeuvring. This is essential to provide a safe flight during the mission operations. Moreover, the limitation in the control effort of the onboard engine is considered, to produce feasible optimal trajectories for the formation. In this work, we consider the case of the station keeping, to maintain the triangular formation of Fig. 1 fixed in time. This is required by the nominal scientific phase of the mission, for remote sensing observation purposes.

4.2 Control algorithms and actuators model

The control algorithm implements the manoeuvre commanded by the guidance algorithms and provides the command control to the actuators. It implements an optimal control to minimize the error between the actual state and the desired state, from the navigation reconstruction and the guidance algorithms, respectively.

In this work, we implement a feedback control law for non-linear system dynamics. This first approach implements the feedback linearisation of the system error dynamics [18]. Starting with the non-linear relative dynamics, we consider the control term introduced by a control matrix $\boldsymbol{B}$:

$$\dot{\boldsymbol{x}}(t) = f(t,\boldsymbol{x}) + \boldsymbol{B}\,\boldsymbol{u}(t) \tag{5}$$

Where the function $f(t,\boldsymbol{x})$ represents the non-linear relative motion and includes the perturbation effects of the mean $J2$ and the drag approximation. The matrix $\boldsymbol{B}$ is selected equal to $\boldsymbol{B} = [\boldsymbol{0_{3,3}};\ \ \boldsymbol{I}_{3,3}]$. At this point we rearrange Eq. (5), to isolate the control term:

$$\boldsymbol{B}^{-1}\dot{\boldsymbol{x}}(t) = \boldsymbol{B}^{-1} f(t,\boldsymbol{x}) + \boldsymbol{u}(t) \tag{6}$$

So that we can define the control law as following, introducing a new equivalent input:

$$\boldsymbol{u}(t) = -\boldsymbol{B}^{-1} f(t,\boldsymbol{x}) + \boldsymbol{B}^{-1}\,\boldsymbol{v}(t) \tag{7}$$

Where $\boldsymbol{v}(t)$ represents the new equivalent input, which is selected from the system error dynamics. The close loop error in the relative dynamics is selected as the difference between the actual relative state $\boldsymbol{x}(t)$ and the desired relative state $\boldsymbol{x}_d(t)$. The actual state comes from the state reconstruction from the navigation filter, while the desired one is obtained from the guidance algorithm: $\boldsymbol{e}(t) = \boldsymbol{x}(t) - \boldsymbol{x}_d(t)$. From the error definition, we recover the equivalent input for Eq. (7):

$$\boldsymbol{v}(t) = -\boldsymbol{k_1}\,\boldsymbol{e}(t) - \boldsymbol{k_2}\,\dot{\boldsymbol{e}}(t) \tag{8}$$

Where k_1 and k_2 are symmetric positive definite feedback gain matrices, which can be computed with several methods, such as the pole placement or the LQR approach. In the global control law, an additional term could be introduced to account for non-linear disturbance force non included in the relative dynamics. This term, $\boldsymbol{n}(t)$ sum up in Eq. (7) to contribute to the closed-loop control.

Consideration should be done for the non-linear relative motion function $f(t,\boldsymbol{x})$. The formation dynamics could be expressed in the RTN frame, considering non-linear equations of motions including the main perturbing effect for LEO satellites [19]. This allows a precise relative motion reconstruction inside the controller, which benefits from the inclusion of the main perturbing effect directly in the dynamics but is time-consuming due to the need of solving a non-linear equation of motion. A different approach could be considered to reduce the computational effort, by introducing linearized equations of motion in the controller. In literature, several studies have introduced a state transition matrix to precisely describe the relative motion under the external perturbation effects [20,21]. In this work, we considered a linear dynamic approximation including the effect of the mean J_2 and the drag perturbation, described in the RTN reference frame [20]. The other perturbing effect of the LEO environment, such as solar radiation pressure or higher-order spherical harmonics, are included in the noise term $\boldsymbol{v}(t)$ to the control law. The schematic representation of the feedback control loop is reported in Fig. 5.

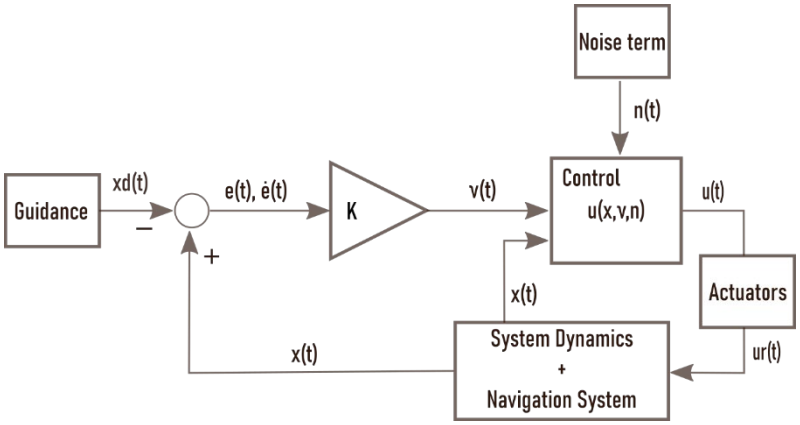

Fig. 4: Schematics of the closed-loop feedback control.

4.2.1 Control actuators

FFLAS is equipped with four low-thrust engines, the QinetiQ T5, used for implementing the manoeuvre and station keeping of the satellites [22]. The thrusters are oriented in the transversal-normal plane, as shown in Fig. 4, where the satellite attitude is assumed to be in the nominal science mode. The GNC simulator proposed in this paper do not implement the control on the attitude of the satellite, but it is assumed that the satellite body frame x_b, y_b, z_b is oriented along the RTN direction, thanks to the on-board reaction wheels actuators. Thus, for our case, we consider $\{x_b, y_b, z_b\}$ aligned with the $\{x, y, z\}$ frame.

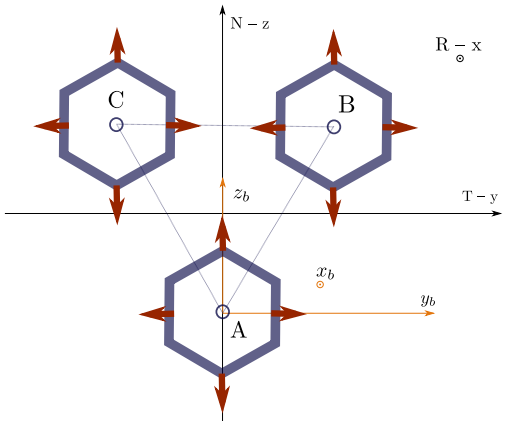

Fig. 5: Orientation of the onboard thruster for the FFLAS formation, with the red arrows.$\{x, y, z\}$ represent the RTN frame, while $\{x_b, y_b, z_b\}$ is the body frame.

After the definition of the ideal control law from Eq. (7), we need to characterise the actual control that the onboard thruster can provide. A real actuator will always introduce a delay in the ideal control, due to the intrinsic time delay in the actuator response. Specifically, the commanded control is elaborated and transmitted by the propulsion control unit to the engine assembly, which has an intrinsic delay in the response time. There exist some strategies to minimise this intrinsic response delay, which could be implemented in a more refined analysis of the actuators control. It can be shown that the total delay time in the control loop model depends on the pure time delay and on the flow filter response time. It is strictly dependent on the actuator type considered. For the case of the QinetiQ T5, we considered a delay time in the control loop of about 5 ms.

Moreover, the thrust noise and the error on the thrust level are implemented in the model to account for the real behaviour of the engine. The inclusion of such values is important to simulate a real scenario for the close loop implementation. During the mission operations, the control would never be the ideal one, but it will be subject to such uncertainties in both modulus and direction. Finally, the thrust is limited to the maximum thrust level that the engine could provide, thanks to a saturation limit. These parameters for the QinetiQ T5 engine are reported in Table 2.

The resulting control thrust given by the actuator is considered in the closed-loop dynamics of the relative motion. Due to the implementation of real performances of the engine, this control effort is not equivalent to the ideal control level but includes the uncertainties typical of a real actuator. This allows to evaluate the proper convergence of the control law also in presence of uncertainties and errors: for this reason, the control should be robust to the resulting relative motion, which accounts for such delays.

Table 2: general QinetiQ T5 performances [22].

Characteristic	**Value**
Thrust error	$\pm$ 5 % for thrust level $<$ 3 mN
	$\pm$ 1 % for thrust level $>$ 3 mN
Thrust noise	1.2 mN/$\sqrt{\text{Hz}}$ at 1 mHz
	0.012 $mN/\sqrt{Hz}$ at 100 Hz
Thrust range	0 to 25 mN

4.3 GNSS-based navigation algorithms

The navigation system aims at estimating the absolute and the relative state of the satellites in the formation. For the FFLAS formation, we consider a decentralized architecture, where the reference satellite computes the absolute state measurement and shares the information with the other satellites in the formation. At this point, each vehicle computes its relative state through a navigation filter. Specifically, the onboard sensors provide measurements on the position and velocity evolution of each satellite during the time. These measurements are subject to noise and disturbances, caused by the sensor's accuracy on the measures. The navigation algorithms are introduced to filter and process such information, to generate a good estimation of the actual state of the satellite. For space application, the typical filter used for absolute and relative state estimation is the Extended Kalman Filter [23]. This is an extension of the Kalman filter for non-linear dynamics representation. The general idea of the EKF is to provide a recursive estimate for the state x_k in time by propagating the current estimate of the state and the error covariance matrix of the state in time. At every time step, we assume the existence of a closed-form expression for the predicted state as a function of the previously estimated state x_k, noise w_k, control u_k, and time t:

$$x_{k+1} = f(x_k, u_k, t) + w_k \tag{9}$$

At this point, the Jacobian of the predicted state can be computed with respect to the previous state as

$$F^x = \frac{\partial f}{\partial x} \tag{10}$$

Once the Jacobian and the predicted state have been computed, the predicted covariance estimate is recovered as function process noise covariance Q_k: $P_{k+1} = F^x P_k F^{x\prime} + Q_k$. A similar procedure is applied to compute the measurement z_k to be estimated by the filter:

$$z_{k+1} = h(x_k, t) + v_k \tag{11}$$

Where v_k is the measurement noise. Similarly, also the Jacobian of the measurement is computed, H^x. Now the update of the state is computed as

$$\begin{aligned} \tilde{y}_{k+1} &= z_{k+1} - h(x_k, t) \\ S_{k+1} &= H_{k+1} P_{k+1} H'_{k+1} + R_k \\ K_{k+1} &= P_{k+1} H_{k+1} S'_{k+1} \\ \hat{x}_{k+1} &= x_{k+1} + K_{k+1}\, \tilde{y}_{k+1} \\ \hat{P}_{k+1} &= (I - K_{k+1} H_{k+1}) P_{k+1} \end{aligned} \tag{12}$$

Where R_k is the observation noise covariance. The estimate of the state $\hat{x}_{k+1}$ is provided together with the covariance matrix $\hat{P}_{k+1}$, which gives an idea of the level of uncertainty in the current estimate. Each term in the covariance matrix represents the square error between the real and the estimated state.

The navigation system aims to obtain an accurate estimate of the relative state of the satellites from raw GNSS measurements. Specifically, as reported in Section 2, accuracy in the order of cm and mm/s are required for the relative state to achieve the desired formation control accuracy. For the FFLAS scenario, the satellites will fly at about 12 m of distance, thus, it is essential to guarantee a precise state reconstruction to provide a safe flight.

The GNSS receivers can provide three different measures: the pseudo-range ρ_{pr}, the carrier phase ρ_{cp}, and the doppler measurement $\dot{\phi}$. The former is the range between the GNSS satellite and the user, in our case one of the satellites of the formation. It is subject to some noises, the receiver clock error, the ionospheric error, and other sources. The second instead, measure the difference between the carrier phase of the GNSS and the receiver satellite, and the doppler measurement provides information on the range rate.

4.3.1 Absolute navigation

The first state estimation is absolute navigation, which is necessary to compute the relative navigation measurement. From the GNSS measurements, the absolute state of a satellite can be estimated using the information on the pseudo-range and the doppler measurements [24]. In this work, we consider the absolute state of each satellite in the formation equal to the position and velocity in the ToD frame, given by the SKiLLeD propagator, and we add noise to the measurement, to account for the sources of uncertainties or noises.

The state vector for each satellite is defined from the inertial position and velocity:

$$x_{ABS} = \{r_j, v_j\}' \tag{13}$$

Where r_j and v_j are defined for the j-th satellite of the formation. Its corresponding dynamics is described with non-linear equations of motion, including the effect of Earth oblateness (J_2) and drag effect. The measured quantities are computed corrupting the inertial ToD position and velocity with a zero-mean Gaussian noise:

$$\begin{aligned} r_{meas} &= r_{ToD} + N(\sigma_r) \\ v_{meas} &= v_{ToD} + N(\sigma_v) \end{aligned} \tag{14}$$

The terms σ_r and σ_v are the standard deviation of the position and velocity noises. These terms represent the measurement vector $y_{ABS} = \{r_{meas}, v_{meas}\}'$. A block diagram can be used to provide an overview of the measurement simulation process, as shown in Fig. 6.

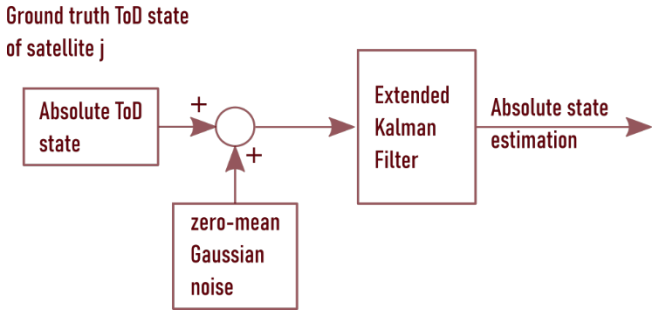

Fig. 6: Schematic of the simulation process for the absolute navigation measurement.

4.3.2 Relative navigation

After the absolute state reconstruction, it is important to recover the relative states between the satellites. The relative state is computed from the GNSS measurements between a couple of satellites in the formation [25]. Between two receivers of two different satellites, i and j, the single difference carrier phase measurement can be computed as:

$$\rho^{ij}_{sdcp}(t) = \rho^{j}_{cp} - \rho^{i}_{cp} \tag{15}$$

This procedure can be applied to any couple of satellites in the formation. Similarly, a single difference among the doppler measurement can be computed to provide the range-rate change in time:

$$\Delta\dot{\phi}^{ij} = \dot{\phi}^{j} - \dot{\phi}^{i} \tag{16}$$

The advantage of using the differential measurement is the cancelling of the ionospheric noise, which affects the GNSS measurements. Moreover, it provides a value with smaller uncertainties and external noises. Now the state vector for the formation can be computed at each time instant as:

$$x_{REL} = \left\{x^{i}_{ABS} \quad x^{1i}_{REL} \quad \dots \quad x^{ji}_{REL} \quad \dots \quad x^{(N-1)i}_{REL}\right\} \tag{17}$$

Where the index i stands for the reference satellite in the formation, and the index j represents the other satellites in the formation for $j = 1{:}\,N-1$, with N the number of vehicles in the formation. The relative state x^{ji}_{REL} represents the position and velocity of satellite j with respect to satellite i. In this work, we start from the absolute state estimation in the ToD frame, and we recover the relative state of the satellite j of the formation with respect to the reference i satellite. The measurement vector is the relative state of the satellites in the formation corrupted by a zero-mean Gaussian noise:

$$\begin{aligned} r^{REL}_{meas} &= r^{ji}_{rel} + N\left(\sigma_{r_{rel}}\right) \\ v^{REL}_{meas} &= v^{ji}_{rel} + N\left(\sigma_{v_{rel}}\right) \end{aligned} \tag{18}$$

The terms σ_r and σ_v are the standard deviation of the position and velocity noises. These terms represent the measurement vector $y_{REL} = \{r_{meas}^{REL}, v_{meas}\}'$. The relative navigation filter is used to estimate the relative position and velocities of the satellites in the formation from the measurement subject to noises, as represented in Fig. 7.

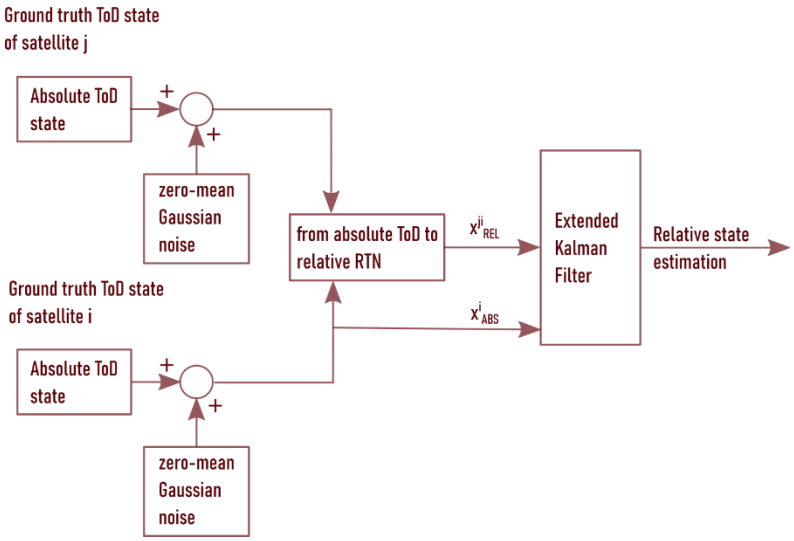

Fig. 7: Schematic of the simulation process for the relative navigation measurement.

4.3.2 Navigation errors

The characterization of the estimation error is essential to evaluate the performances of the navigation filter. The state estimation error can be computed at each time step by subtracting the actual and the estimated state:

$$e_{NAV}(t_k) = x(t_k) - \hat{x}(t_k) \tag{19}$$

Another parameter to assess the state estimation performances is the standard deviation, from the filter covariance matrix P_k:

$$\sigma_k = \sqrt{P_k} \tag{20}$$

Both the navigation error and the standard deviation provide a performance of the navigation solution with respect to the actual state at each time instant.

5. Science mode simulation results

This section describes the results of the simulations for formation flying maintenance of the FFLAS mission study. This paper focuses on the preliminary results of the GNC simulator for the formation maintenance during the scientific mode, for Earth observation purposes.

5.1 FFLAS science mode

The description of the FFLAS mission study has been presented in Section 2. The science mode represents the nominal mission phase when all the satellites are in Earth Pointing Mode for remote sensing analysis. During this phase, the triangular formation of the satellites should lie on the transversal-normal plane of the RTN, to maintain the normal to the payload parallel to the radial direction. In this phase a three-axis stabilizing attitude control should be implemented, to maintain the body frame aligned with the RTN, as shown in Fig. 5.

The aim of the navigation system is the reconstruction of the real-time absolute and relative state of the satellites, filtering out the noise present in the GNSS sensor measurement. These estimations are then used in the controller to provide the commanded control effort to the onboard actuator.

We consider that each satellite has four low thrust actuators onboard, oriented in the transversal and normal direction (see Fig. 5). The attitude of the satellite is considered controlled by the onboard attitude actuators (reaction wheels and magnetic torquers), to maintain the Earth pointing direction and the solar panels in the sun pointing

direction, to ensure proper power production for the satellite system. Finally, an inter-satellite link is exploited to exchange continuously data on the absolute and relative state of the satellites to monitor the inter-satellite collision avoidance and to improve the state reconstruction from GNSS measurements.

5.2 FFLAS Simulation Settings

This section describes the settings used for the simulation scenario. The simulations are based on MATLAB/Simulink® R2021a, operating on an Intel® Core™ i7-7700, 3.60 GHz processor.

The orbital scenario is simulated three times the orbital period, for a preliminary evaluation of the GNC performances. This period is enough to introduce the nonlinearity of the relative dynamics and to analyse the convergence of the controller and the navigation filter. We considered the gravity field due to the gravitation harmonics up to a 6x6 order, and the influence of drag during the motion. The time step was selected equal to 1.0 s to provide the velocity vector as the rate of change of the position vector in 1-second. The main parameter for initializing the simulation are reported in Table 3.

Table 3: Simulation setting for the science mode.

Options	**Settings**
Simulation duration	5 hrs 6 min (3 orbital periods)
Orbital perturbations	Gravity field (6x6), Drag (MSISE)
Timestep	1.0 sec

The feedback linearization controller requires the definition of the control gain. After a parametric analysis, the values of -0.1 and -0.004 are selected for the gains k_1 and k_2 in Eq. (8). Moreover, for the FFLAS satellites, a mass of about 1700 kg is considered for the computation of the thrust level.

Finally, for the navigation system, the performances of the RUAG Leorix GNSS receiver* is considered in the simulation. The main parameters useful to set up the EKF are reported in Table 4.

The initial states of the FFLAS satellites are reported in Table 4, where the relative position is expressed in the RTN frame for each satellite with respect to the central virtual point of the triangular formation. The science mode geometry is shown in Fig. 5, where A, B, and C represents the satellite of the formation and O is the central virtual point. The initial conditions in the RTN frame were computed from the representation in the inertial ToD frame, which also considers the effect of nutation and precession.

Table 4: Controller and navigation setting for the science mode simulation.

Guidance	**Values**
Reference SSO orbit	$\{7.1531 \times 10^6$ m $\quad 6.4e \times 10^{-4} \quad 2.114$ rad $\quad 3.434$ rad $\quad 3.36$ rad$\}$
Sat A	$\{-1.9 \times 10^{-3} \quad 6.5 \times 10^{-3} \quad -5.369 \quad 0 \quad 0 \quad 0\}'$ m, m/s
Sat B	$\{-1.9 \times 10^{-3} \quad 6.236 \quad 5.369 \quad 0 \quad 0 \quad 0\}'$ m, m/s
Sat C	$\{-1.9 \times 10^{-3} \quad -6.236 \quad 5.369 \quad 0 \quad 0 \quad 0\}'$ m, m/s
Control	
Control gain	-0.1 and -0.004
Satellite mass	1700 kg
Navigation	
Error in the position	1.0 m 3D rms
Error in the velocity	2 mm/s 3D rms
Carrier phase error	< 1.8 mm rms
Code measurement error	< 0.7 mm rms

* https://www.ruag.com/en/products-services/space/electronics/navigation-receivers-signal-processing-0

5.3 FFLAS science mode simulation results

This section describes the results of the simulations performed for the science mode of the FFLAS mission study. The simulation has the following objectives:

- Maintains the formation geometry fixed and rigid, for a correct functioning of the payload,
- Provides a baseline of the trust level required to control the formation,
- Provides a preliminary performance evaluation of the navigation filter.

The simulator provides the control effort to maintain the satellites on their triangular formation geometry. The evolution of the relative motion with respect to the reference virtual point of the formation is reported in Fig. 8. It shows both the evolution in the ROEs framework and the RTN frame. The three satellites in the formation, A, B, and C, are represented with three different colours in the figures: red, green, and blue, respectively. In the ROEs evolution, the effect of the control is evident on the time evolution of the relative argument of latitude $\delta\lambda$, which is forced to remain constant in time, maintaining the formation geometry fixed. This behaviour can be observed also in the RTN representation, where the evolution in the transversal and normal plane remains constant in time. A small variation in the radial component is present and must be accounted for in a more refined analysis.

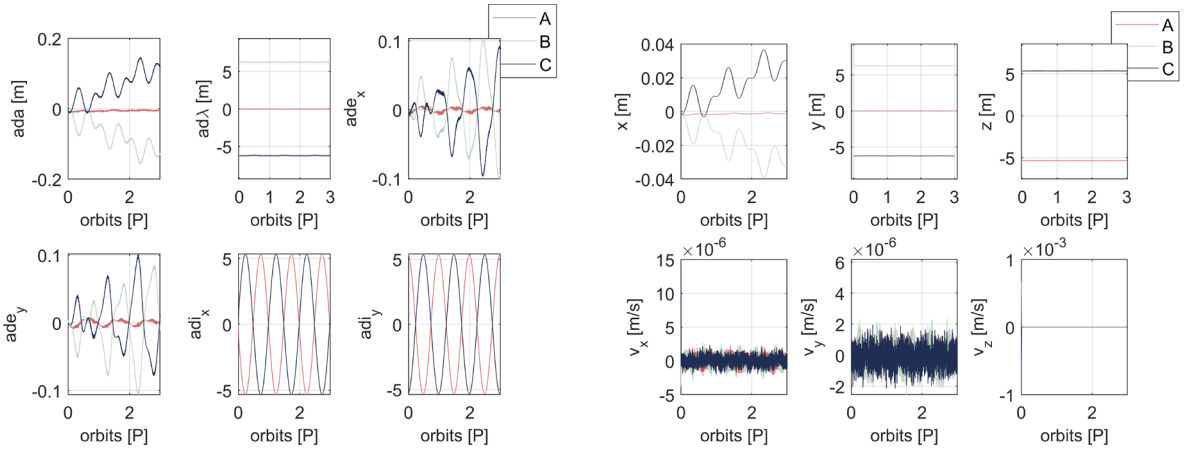

Fig. 8: Relative motion evolution of the FFLAS satellites during the science mode in ROEs (left) and RTN (right) frame.

5.3.1 Relative state reconstruction

The performances of the relative state reconstruction by the EKF have evaluated thanks to the relation in Eq. (19). This relation provides a measurement of the separation between the estimated and actual relative position and velocity. A small variation is an indication of the accuracy of the navigation system. For the FFLAS formation, the following real-time navigation accuracies are required:

- Relative position accuracy in the order of a centimetre
- Relative velocity accuracy in the order of micro-centimetre per second.

The results from the simulation of the science mode are shown in Fig. 9. On the left, the relative state reconstruction is reported for the three satellites A, B, and C. By comparing it with the reference state in Fig. 8, it shows a similar behaviour, including the noise due to the filter reconstruction of sensor measurements. GNSS information is subject to several noises and uncertainties sources, and proper data manipulation is required to produce an accurate estimation.

The navigation error is shown in the right part of Fig. 9, where both the error in the relative position and velocity is reported in the RTN frame. The error in the reconstruction of the relative position remains under the ± 2 cm level, for all the directions. On the other hand, the error in the relative position reconstruction is in the order of $5 \cdot 10^{-3}$ cm/s. This is an important preliminary result, that confirms the accuracy of the GNSS-based navigation. A more accurate and robust solution can be obtained by adding in the filter the information on the relative position among the satellites given by an optical sensor. Optical sensors provide very accurate measurements of the range and range rate, and their inclusion in the simulator is envisioned for a more robust characterization of the navigation performances.

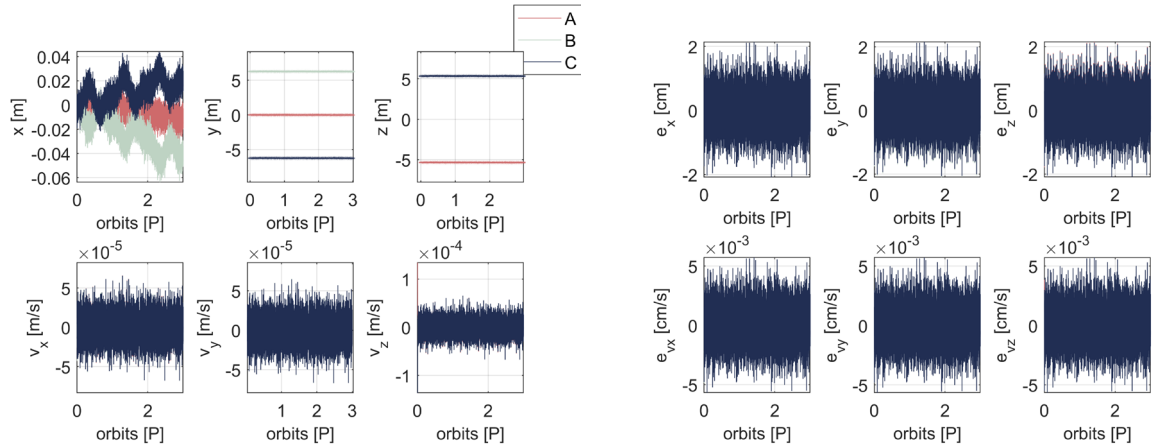

Fig. 9: Relative state reconstruction performances for the navigation system. Relative position and velocity (left) and state estimation error (right).

5.3.2 Performances of the controller

The feedback linearization controller implements error-based feedback control to maintain the formation keeping. The performances of the controller are evaluated to assess the error in the position and velocity control for each satellite. Ideally, the accuracy should be in the same order as the navigation accuracy (cm-level), and it is always bigger or equal to it.

For the science mode of the FFLAS mission study, the performances of the controller are shown in Fig. 10. The control accuracy is reported on the left, where the error between the actual relative position and velocity with respect to the reference value from the guidance analysis remains small, in the order of few centimetres. In particular, the control error on the relative position is about 2 to 6 cm, while the one for the relative velocity is around 5×10^{-3} cm/s. This is a good result for this preliminary analysis, which guarantee the correct formation geometry maintenance. Consequently, at each time instant, the inter-satellite distance for the formation remains stable around its initial condition of 12.4 m, as shown in Fig. 10 (right).

Finally, the control thrust provided by the onboard low thrust engines is reported in Fig. 11. Both the thrust in the inertial and the relative RTN frame are reported on the left and right of the figure, respectively. The control in the RTN corresponds to the control effort in the body frame, aligned with the thrusters in the transversal and normal plane. The thrust is limited to $\pm$ 25 mN, due to the technological performances of the QinetiQ T5, (see Section 4.2).

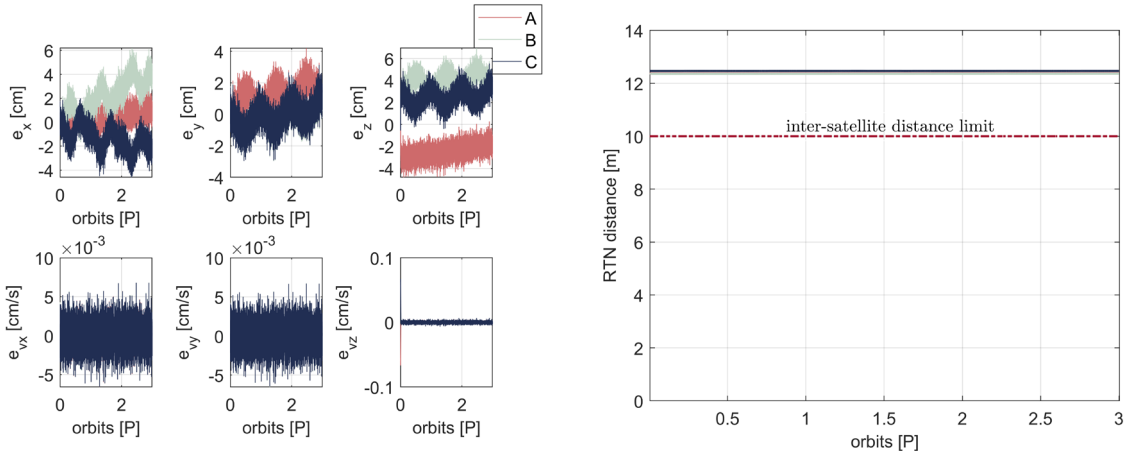

Fig. 10: Performances of the controller for the formation keeping. Control accuracy (left) and real-time inter-satellite distance evaluation (right)

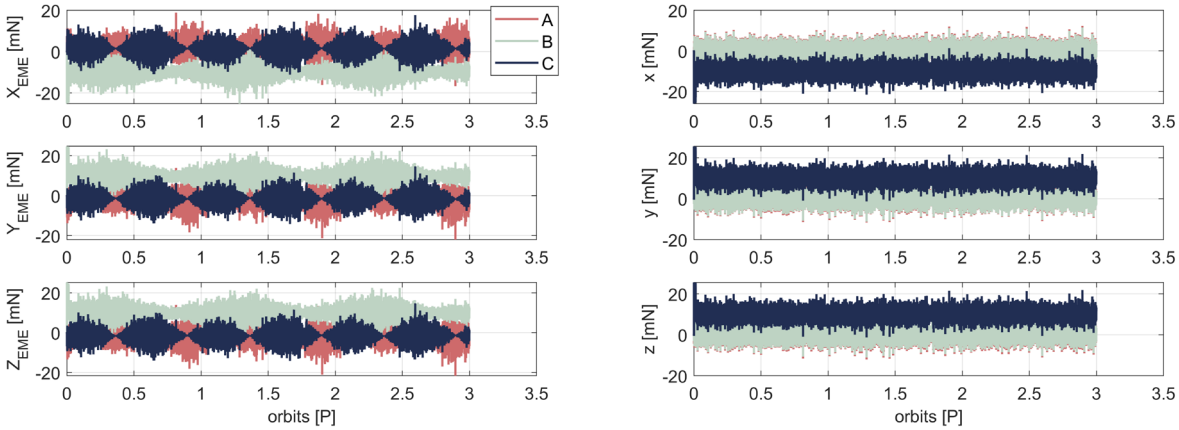

Fig. 11: Control thrust provided by the onboard actuators in the inertial frame $\{X_{EME}, Y_{EME}, Z_{EME}\}$ (left) and in the relative RTN frame $\{x, y, z\}$ aligned with the body frame (right).

6. Conclusions

This paper provides a simulator of guidance, navigation and control for multiple-satellite formation flying. It relies on a high-fidelity dynamical propagator, based on a C++ environment, and provide a baseline for the controller and the navigation filter to be included in the closed-loop dynamics. The scenario considered the FFLAS formation on a quasi-circular SSO orbit in the LEO environment. Consequently, the main perturbing effects have been considered in the dynamical propagator, such as the Earth's oblateness and the drag effect, while the solar radiation pressure and the third body perturbations are included in the propagation noise.

The relative navigation problem based on the GNSS sensor is presented, for the estimation of the relative position and velocity states. A preliminary result of the performances of the EKF is discussed for the analysis case, providing the navigation error in the relative state reconstruction of each satellite in the formation. However, the performances of the EKF strongly depends on the selected onboard dynamic and the sensor performances (noise and covariance). For this reason, accurate analysis on the robustness of the filter will be performed as part of the study for the FFLAS mission design.

Moreover, a first approach for the controller is presented, based on feedback linearization error. Other approaches could be considered for more accurate control of the system dynamics, which could better include the nonlinearities and uncertainties in the system.

To conclude, a preliminary evaluation of the GNC simulator is presented in this work, to demonstrate the feasibility of the FFLAS formation flying during the scientific phase of the mission operations. Future development will be the extension of the GNC simulator for the other nominal and non-nominal mission operations, starting from the injection by the launcher, to the end-of-life disposal at the end of the mission life.

Acknowledgements

The work presented in this paper was co-founded by the European Space Agency (Contract No. 4000128576/19) and by the European Research Council (ERC) under the European Unions Horizon 2020 research and innovation program (grant agreement No. 679086 COMPASS). The view expressed in this paper can in no way be taken to reflect the official opinion of the European Space Agency.

The contribution of Dr Gabriella Gaias is funded by the European Union's Horizon 2020 research and innovation program under the Marie-Sklodowska Curie grant ReMoVE (grant agreement No. 793361).

The authors would like to acknowledge Dr Miguel Piera's support, from Airbus Space Espana, leading the contract.

References

[1] A.M. Zurita, I. Corbella, M. Martin-Neira, M.A. Plaza, F. Torres, F.J. Benito, Towards a SMOS operational mission: SMOSOps-Hexagonal, IEEE Journal of Selected Topics in Applied Earth Observations and Remote Sensing. 6 (2013) 1769–1780. https://doi.org/10.1109/JSTARS.2013.2265600.

[2] M. Martì-Neira, A. Zurita, M.A. Plaza, J. Benito, SMOS Follow-on Operational Mission Concept (SMOSops-H), in: 2nd SMOS Science Conference, 2015.

[3] M. Martin-Neira, M. Suess, N. Karafolas, P. Piironen, F. Deborgies, A. Catalan, R. Vilaseca, J. Montero, M. Puertolas, D. Outumuro, I. Corbella, I. Duran, N. Duffo, R. Materni, T. Mengual, M.A. Piqueras, A. Olea, A. Solana, J. Closa, A. Zurita, J.I. Ramirez, O. Breinbjerg, J.M. Bjorstorp, K. Kaslis, S.S. Kristensen, R. Oliva, R. Onrubia, A. Camps, J. Querol, Technology Developments for an Advanced L-Band Radiometer Mission, in: International Geoscience and Remote Sensing Symposium (IGARSS), Institute of Electrical and Electronics Engineers Inc., 2020: pp. 6507–6510. https://doi.org/10.1109/IGARSS39084.2020.9324378.

[4] F. Scala, G. Gaias, C. Colombo, M. Martìn-Neira, Formation flying l-band aperture synthesis: Design challenges and innovative formation architecture concept, in: Proceedings of the International Astronautical Congress, IAC, 2020.

[5] G. Di Mauro, M. Lawn, R. Bevilacqua, Survey on guidance navigation and control requirements for spacecraft formation-flying missions, Journal of Guidance, Control, and Dynamics. 41 (2018) 581–602. https://doi.org/10.2514/1.G002868.

[6] Z. Kang, B. Tapley, S. Bettadpur, J. Ries, P. Nagel, R. Pastor, Precise orbit determination for the GRACE mission using only GPS data, Journal of Geodesy. 80 (2006) 322–331. https://doi.org/10.1007/s00190-006-0073-5.

[7] S.D. Amico, E. Gill, M. Garcia, O. Montenbruck, GPS-Based Real-Time Navigation for the PRISMA Formation Flying Mission, in: 3rd ESA Workshop on Satellite Navigation User Equipment Technologies (NAVITEC), ESA, Noordwijk, The Netherlands, 2006: pp. 11–13.

[8] O. Montenbruck, M. Wermuth, R. Kahle, GPS based relative navigation for the Tan DEM-X mission - First flight results, Navigation, Journal of the Institute of Navigation. 58 (2011) 293–304. https://doi.org/10.1002/j.2161-4296.2011.tb02587.x.

[9] J.K. Eyer, C.J. Damaren, R.E. Zee, E. Cannon, A formation flying control algorithm for the CanX-4&5 low earth orbit nanosatellite mission, in: International Astronautical Federation - 58th International Astronautical Congress 2007, 2007: pp. 3827–3838.

[10] G. Gaias, S. D'Amico, The Autonomous Vision Approach Navigation and Target Identification (AVANTI) Experiment : Objectives and Design, GNC 2014: 9th International ESA Conference on Guidance, Navigation & Control Systems, Porto, Portugal. (2014).

[11] O. Montenbruck, E. Gill, F. Lutze, Satellite Orbits: Models, Methods, and Applications, Applied Mechanics Reviews. 55 (2002) B27. https://doi.org/10.1115/1.1451162.

[12] G.W. Hill, Researches in the Lunar Theory, American Journal of Mathematics. 1 (1878) 5–26.

[13] S. D'Amico, Relative Orbital Elements as Integration Constants of Hill's Equations, (2005) 3–12.

[14] B. Tapley, J. Ries, S. Bettadpur, D. Chambers, M. Cheng, F. Condi, B. Gunter, Z. Kang, P. Nagel, R. Pastor, T. Pekker, S. Poole, F. Wang, GGM02 - An improved Earth gravity field model from GRACE, Journal of Geodesy. 79 (2005) 467–478. https://doi.org/10.1007/s00190-005-0480-z.

[15] J.M. Picone, A.E. Hedin, D.P. Drob, A.C. Aikin, NRLMSISE-00 empirical model of the atmosphere: Statistical comparisons and scientific issues, Journal of Geophysical Research: Space Physics. 107 (2002) SIA 15-1-SIA 15-16. https://doi.org/10.1029/2002JA009430.

[16] D. Morgan, S.J. Chung, F.Y. Hadaegh, Model predictive control of swarms of spacecraft using sequential convex programming, in: Journal of Guidance, Control, and Dynamics, American Institute of Aeronautics and Astronautics Inc., 2014: pp. 1725–1740. https://doi.org/10.2514/1.G000218.

[17] F. Scala, G. Gaias, C. Colombo, M. Martin-Neira, Three Satellites Formation Flying: Deployment and Formation Acquisition Using Relative Orbital Elements, in: 2020 AAS/AIAA Astrodynamics Specialist Conference, Lake Tahoe, CA, USA, 9-12 Aug., 2020: pp. 1-17 (AAS 20-625).

[18] J.J.E. Slotine, J. Karl Hedrick, Robust input-output feedback linearization, International Journal of Control. 57 (1993) 1133–1139. https://doi.org/10.1080/00207179308934435.

[19] G. Xu, D. Wang, Nonlinear dynamic equations of satellite relative motion around an oblate earth, Journal of Guidance, Control, and Dynamics. 31 (2008) 1521–1524. https://doi.org/10.2514/1.33616.

[20] M. Sabatini, G.B. Palmerini, Linearized formation-flying dynamics in a perturbed orbital environment, IEEE Aerospace Conference Proceedings. (2008). https://doi.org/10.1109/AERO.2008.4526271.

[21] G. Gaias, J.S. Ardaens, O. Montenbruck, Model of J2 perturbed satellite relative motion with time-varying differential drag, Celestial Mechanics and Dynamical Astronomy. 123 (2015) 411–433. https://doi.org/10.1007/s10569-015-9643-2.

[22] C.H. Edwards, N.C. Wallace, C. Tato, P. Van Put, The T5 ion propulsion assembly for drag compensation on GOCE, in: European Space Agency, (Special Publication) ESA SP, 2004: pp. 217–223.

[23] D. Simon, Optimal state estimation: Kalman, H∞, and nonlinear approaches, 2006. https://doi.org/10.1002/0470045345.

[24] J.I. Park, H.E. Park, S.Y. Park, K.H. Choi, Hardware-in-the-loop simulations of GPS-based navigation and control for satellite formation flying, Advances in Space Research. 46 (2010) 1451–1465. https://doi.org/10.1016/j.asr.2010.08.012.

[25] S. Leung, O. Montenbruck, Real-time navigation of formation-flying spacecraft using global-positioning-system measurements, Journal of Guidance, Control, and Dynamics. 28 (2005) 226–235. https://doi.org/10.2514/1.7474.